Influence of the Discretization Method on the Integration Accuracy of Observers with Continuous Feedback

Mihai Comanescu, IEEE Member
Penn State Altoona, 3000 Ivyside Park, Altoona, PA

Abstract – **The paper discusses the problem of integrating the equations of state observers associated with direct field orientation (DFO) of motor drives and studies the influence of the discretization method used on the accuracy of integration. In a typical implementation, discrete-time integration is done using Euler's discretization method (forward rectangular rule) – the method is simple and integration is accurate when the drive operates at low and medium speed. However, as the frequency increases, the integration becomes inaccurate because the Euler approximation starts losing more and more area from under the curve. Theoretically, the problem could be alleviated by increasing the sampling frequency; however, this cannot always be done. Another idea would be to adopt a more accurate (but more computationally intensive) integration method, for example, trapezoidal integration (Tustin method). The paper shows that, at high frequency, under ideal conditions, trapezoidal integration performs better than the Euler method. In a real implementation, however, conditions are non-ideal since the measured signals bring dc offsets and imperfections into the terms to be integrated – as a result, pure integration must be replaced with quasi-low pass filtering. Under these conditions, the paper compares the Euler, Tustin and backward rectangular methods from the point of view of integration accuracy. The implications related to direct field orientation of motor drives are studied by considering a full-order observer for the PMSM – this is discretized using the three methods considered and the results are compared. At high frequency, neither integration method gives perfect results; the Euler method yields a waveform that leads the expected one while the backward rectangular method yield a waveforms that lags it. The paper finds that, surprisingly, when quasi-low pass filtering is used, the Tustin method is not significantly more accurate than the other ones – the waveform obtained lags the expected one by an angle comparable with the lead angle of the Euler method. It is shown that the integration accuracy depends on the frequency, sampling time, filter bandwidth and on the integration method used. Accurate high frequency drive DFO control would require correction of the magnitude/phase of the estimates.**

Keywords: **discrete-time integration, Euler method, forward rectangular rule, Tustin method, trapezoidal integration, backward rectangular rule, permanent magnet synchronous motor, rotor position estimation, state observers.**

I. INTRODUCTION

Direct Field Orientation (DFO) is a well-known estimation method used to obtain the rotor position needed for field oriented control of ac motor drives [1]-[4], [5]-[7]. The method is widely used to secure field orientation in sensorless schemes for the permanent magnet synchronous motor and for the induction motor [8]-[15]. In DFO, the rotor position angle (angle of the rotor flux) is obtained using the tan^{-1} function of the stationary reference frame fluxes or EMF components of the motor. Generally, an observer is used to estimate these quantities. Full-order observers [16][17], reduced-order observers [18]-[20], sliding mode observers [21]-[23] or the Extended Kalman Filter can be used [24][25]. Since the observer is constructed based on the motor's model in the stationary reference frame, all the quantities involved (voltages, currents, fluxes, EMFs etc) are theoretically sinusoidal quantities. Implementation of the observer requires (at a minimum) to measure the voltages and currents. With the sensors and interfacing circuitry involved in a typical motor drive, the measured quantities (which should theoretically be sinusoidal) appear in the controller corrupted by dc offsets, distorted, nonsinusoidal and usually containing noise. As a result, when the observer equations are integrated, to avoid the output divergence, the integrators must be replaced by quasi-low pass filters [26][27].

From the point of view of the integration process, given a function (curve) $x(t)$ whose integral must be obtained, the discrete-time integration methods available implement an approximation to computing the area underneath the curve [28]. For example, the Euler method obtains the integral by successively adding rectangular areas – each area is of the form $x_i T_S$ (note that, at sampling time k, the last area added to the integral is $x_{k-1}T_S$). Similarly, the backward rectangular rule computes the area under the curve also based on rectangles; the difference is that at sampling time k, the last area added to the integral is $x_k T_S$, thus, the rectangles extend "backwards" towards the previous samples of $x(t)$. However, the backward rectangular rule is rarely used since it can produce unstable discrete-time filters.

Finally, the trapezoidal method (Tustin method) computes the integral by using trapezes whose areas are of the form $\frac{T_S}{2}(x_{k-1} + x_k)$. From an intuitive point of view, the trapezoidal method seems to be more accurate compared to the other ones since this approximation loses the smallest amount of area from under the curve. However, if the sampling time is sufficiently small, the loss of area is small no matter what integration method is used. With small sampling

time, both the Euler method and the backward rectangular method perform very well too and the extra-accuracy of the trapezoidal method does not produce a significant advantage.

As a result, it is standard to use Euler's method for discrete-time integration since this provides a simpler implementation (simpler calculations and less variables stored from one sampling time to the next) and always gives a stable discrete-time filter. Note that most application notes and real-time software available from the vendors of digital signal processors are developed using this approach [29].

In a real implementation of a three-phase DFO motor drive that requires integration of observer equations, the system's sampling time must be selected based on several performance criteria and constraints. A significant one comes from the fact that the sampling frequency of the control algorithm is very often equal to the switching frequency of the inverter (this is the case when the drive is controlled with a single interrupt). As a result, the sampling frequency cannot be very high since this would require the semiconductor devices to switch very fast. Therefore, if there are accuracy problems related to the discrete-time integration, it may not be possible to reduce the sampling time. Note that in a typical motor drive implementation, the signals are measured by periodic sampling (the sampling time is constant); also, a typical switching frequency is in the range of 1 to 20 KHz.

When the signals to be integrated are of low and medium frequency, Euler based integration works very well. With the state observers associated with DFO, the signals to be integrated are sinusoidal (theoretically) – they correspond to the stationary reference frame quantities of the motor.

However, as the frequency of these signals (and the speed of the drive) increase, Euler integration becomes inaccurate. This is because the loss of area from under the curve becomes more and more significant (another explanation is that the ratio between the sampling frequency and the signal's frequency is not high enough).

The paper shows that, at high frequency, under ideal conditions, the trapezoidal integration method performs better than the Euler method – integration is accurate and the expected signals are obtained. However, when quasi-low pass filters are used instead of ideal integrators, the accuracy expected from the trapezoidal method is not maintained. The paper finds that, at high frequency, the Euler method yields a signal that is leading the expecting signal, the trapezoidal integration yields a signal that lags it; however, the phase errors are comparable.

The paper also investigates the performance of the backward rectangular rule under the same conditions (high frequency and quasi-low pass filtering) – the signal obtained lags the expected signal by an angle even bigger than that obtained with the trapezoidal method.

The PMSM and an associated full-order observer are used as an example of DFO. The equations of this observer are integrated with the Euler, Tustin and backward rectangular method and the integration accuracy is compared.

II. CHARACTERISTICS OF DISCRETE-TIME INTEGRATION METHODS

In discrete-time control, integration and discretization are equivalent. As explained, if the function $x(t)$ is to be integrated in discrete-time, this is done by calculating (approximating) the area under the curve. The three methods considered in this paper are the Euler method (forward rectangular rule), the Tustin method (trapezoidal integration) and the backward rectangular rule. These three approximations to the integral are shown in Fig.1.

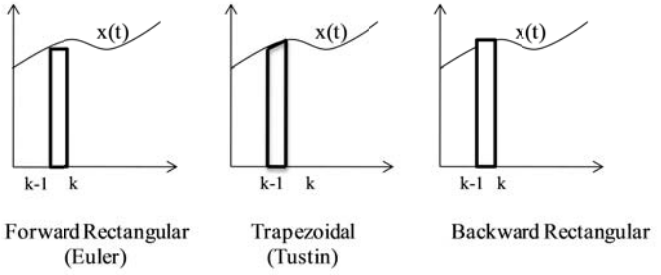

Fig. 1. Discrete-time integration based on the Euler, Tustin and backward rectangular methods

Corresponding to Fig. 1, Table I gives the expressions of the areas (at sampling time k) that correspond to the three integration methods.

TABLE I – APPROXIMATION OF AREAS WITH THE THREE INTEGRATION METHODS

Method	Area (A)
Forward Rectangular Rule (Euler)	$A(k) = A(k-1) + x_{k-1}T_S$
Trapezoidal method (Tustin method)	$A(k) = A(k-1) + \frac{T_S}{2}(x_{k-1}+x_k)$
Backward Rectangular Rule	$A(k) = A(k-1) + x_k T_S$

Considering the transition from continuous-time to discrete-time, Table II gives the discrete-time transfer functions.

TABLE II – CONTINUOUS TO DISCRETE-TIME EQUIVALENTS

Method	Discrete equivalent
Forward Rectangular Rule (Euler)	$\frac{1}{s} \rightarrow \frac{T_S}{z-1}$
Trapezoidal method (Tustin method)	$\frac{1}{s} \rightarrow \frac{T_S}{2}\frac{z+1}{z-1}$
Backward Rectangular Rule	$\frac{1}{s} \rightarrow \frac{T_S z}{z-1}$

Finally, when the equations of observers with continuous feedback are integrated, the pure integrators must be replaced

with quasi-low pass filters ($\frac{1}{s}$ is replaced with $\frac{1}{s+B}$); B is the bandwidth of the filter.

Table III shows the continuous to discrete-time correspondence of the transfer functions with the integration methods considered, when quasi-low pass filtering is used. These transfer functions will be used to integrate the equations of the observer studied.

TABLE III – CONTINUOUS TO DISCRETE-TIME EQUIVALENCE OF QUASI-LOW PASS FILTERS

Method	Discrete equivalent
Forward Rectangular Rule (Euler)	$\frac{1}{s+B} \rightarrow \frac{T_S}{z-(1-BT_S)}$
Trapezoidal method (Tustin method)	$\frac{1}{s+B} \rightarrow \frac{T_S}{2}\frac{z+1}{\left(1+\frac{BT_S}{2}\right)z-\left(1-\frac{BT_S}{2}\right)}$
Backward Rectangular Rule	$\frac{1}{s+B} \rightarrow \frac{T_S z}{(1+BT_S)z-1}$

III. MODELING OF PMSM AND DESIGN OF A FULL-ORDER OBSERVER FOR THE PMSM

To develop the model of the PMSM, consider the flux components $\lambda_{PM\alpha}, \lambda_{PM\beta}$ which are obtained by projecting the PM flux vector on the stationary reference frame. They are:

$$\begin{cases} \lambda_{PM\alpha} = \lambda_{PM} cos\theta \\ \lambda_{PM\beta} = \lambda_{PM} sin\theta \end{cases} \quad (1)$$

where $\theta = \omega_e t$ is the rotor position angle and $\lambda_{PM} = K_E$ (whereK_E is the EMF constant).

The EMFs e_α, e_β of the PMSM are defined as the derivatives of the permanent magnet fluxes:

$$\begin{cases} e_\alpha = p\lambda_{PM\alpha} = -K_E \omega_e sin\theta \\ e_\beta = p\lambda_{PM\beta} = K_E \omega_e cos\theta \end{cases} \quad (2)$$

For sinusoidal PMSM machines constructed with rotor mounted magnets, the flux produced by the stator winding sees a large effective airgap. Since the magnetic material has low permeability, the effective airgap seen by the stator winding consists of the mechanical airgap plus the thickness of the magnet; as a result, the armature reaction is small and these machines have low inductance. On the other hand, the magnets are relatively heavy which increases the inertia of the rotor, resulting in a wide separation between the electrical and the mechanical time constants of the machine. It is therefore quite reasonable to consider that the speed of the motor varies much slower than the electrical quantities ($\dot{\omega}_e \approx 0$). To complete the model of the PMSM, the EMFs in (2) are differentiated with this assumption.

When the stator equations are included, the model of the PMSM with respect to the currents and EMFs is:

$$\begin{cases} pe_\alpha = -\omega_e e_\beta \\ pe_\beta = \omega_e e_\alpha \\ pi_\alpha = -\frac{R}{L} i_\alpha - \frac{1}{L} e_\alpha + \frac{1}{L} V_\alpha \\ pi_\beta = -\frac{R}{L} i_\beta - \frac{1}{L} e_\beta + \frac{1}{L} V_\beta \end{cases} \quad (3)$$

In matrix form, this can be written as:

$$p\begin{bmatrix} e_\alpha \\ e_\beta \\ i_\alpha \\ i_\beta \end{bmatrix} = \begin{bmatrix} 0 & -\omega_e & 0 & 0 \\ \omega_e & 0 & 0 & 0 \\ -\frac{1}{L} & 0 & -\frac{R}{L} & 0 \\ 0 & -\frac{1}{L} & 0 & -\frac{R}{L} \end{bmatrix} \begin{bmatrix} e_\alpha \\ e_\beta \\ i_\alpha \\ i_\beta \end{bmatrix} + \begin{bmatrix} 0 & 0 \\ 0 & 0 \\ \frac{1}{L} & 0 \\ 0 & \frac{1}{L} \end{bmatrix} \begin{bmatrix} V_\alpha \\ V_\beta \end{bmatrix} \quad (4)$$

With the currents as measured quantities, the output equations are:

$$\begin{bmatrix} i_\alpha \\ i_\beta \end{bmatrix} = \begin{bmatrix} 0 & 0 & 1 & 0 \\ 0 & 0 & 0 & 1 \end{bmatrix} [e_\alpha \quad e_\beta \quad i_\alpha \quad i_\beta]^T \quad (5)$$

Based on (4) and (5), a full-order observer can be designed to estimate the states of the PMSM model – this observer is designed based on continuous feedback of the current errors. Using linear observer design methods, the equations are:

$$p\begin{bmatrix} \hat{e}_\alpha \\ \hat{e}_\beta \\ \hat{\imath}_\alpha \\ \hat{\imath}_\beta \end{bmatrix} = \begin{bmatrix} 0 & -\omega_e & 0 & 0 \\ \omega_e & 0 & 0 & 0 \\ -\frac{1}{L} & 0 & -\frac{R}{L} & 0 \\ 0 & -\frac{1}{L} & 0 & -\frac{R}{L} \end{bmatrix} \begin{bmatrix} \hat{e}_\alpha \\ \hat{e}_\beta \\ \hat{\imath}_\alpha \\ \hat{\imath}_\beta \end{bmatrix} + \begin{bmatrix} 0 & 0 \\ 0 & 0 \\ \frac{1}{L} & 0 \\ 0 & \frac{1}{L} \end{bmatrix} \begin{bmatrix} V_\alpha \\ V_\beta \end{bmatrix} + + \begin{bmatrix} l_{11} & l_{12} \\ l_{21} & l_{22} \\ l_{31} & l_{32} \\ l_{41} & l_{42} \end{bmatrix} \begin{bmatrix} \bar{\imath}_\alpha \\ \bar{\imath}_\beta \end{bmatrix} \quad (6)$$

where gains l_{11} through l_{42} should be designed and the current errors are:

$$\begin{bmatrix} \bar{\imath}_\alpha \\ \bar{\imath}_\beta \end{bmatrix} = \begin{bmatrix} \hat{\imath}_\alpha \\ \hat{\imath}_\beta \end{bmatrix} - \begin{bmatrix} i_\alpha \\ i_\beta \end{bmatrix} \quad (7)$$

In the development of the observer, the voltages V_α, V_β and currents i_α, i_β are measured; the speed ω_e is considered known. Since matrix A is time-varying (depends on ω_e) the observer gains are designed based on Lyapunov's nonlinear stability method. They are:

$$\begin{cases} l_{11} = l_{22} = \frac{1}{L} \\ l_{12} = l_{21} = 0 \\ l_{32} = l_{41} = 0 \\ l_{31} = l_{42} = -k \end{cases} \quad (8)$$

where k is a design parameter, $k > 0$. A comprehensive stability analysis and the step by step design procedure for the gains of this observer can be found in [x].

With the gains (8), the equations of this observer are:

$$\begin{cases} p\hat{e}_\alpha = -\omega_e \hat{e}_\beta + \frac{1}{L}\bar{\imath}_\alpha \\ p\hat{e}_\beta = \omega_e \hat{e}_\alpha + \frac{1}{L}\bar{\imath}_\beta \\ p\hat{\imath}_\alpha = -\frac{R}{L}\hat{\imath}_\alpha - \frac{1}{L}\hat{e}_\alpha + \frac{1}{L}V_\alpha - k\bar{\imath}_\alpha \\ p\hat{\imath}_\beta = -\frac{R}{L}\hat{\imath}_\beta - \frac{1}{L}\hat{e}_\beta + \frac{1}{L}V_\beta - k\bar{\imath}_\beta \end{cases} \quad (9)$$

In the paper, this observer is used to study the accuracy of the integration methods considered.

IV. SIMULATION RESULTS

Simulations are done using the Matlab/Simulink package. The parameters of the PMSM used are shown in Table IV.

TABLE IV – PMSM PARAMETERS

Stator resistance	R	2.5 Ω
Synchronous inductance	L	1.8 mH
Rated voltage	V_n	18.2 V
Rated continuous torque	T_C	50 oz-in
Rated speed	n	6000 rpm
Number of poles	P	4

The simulation model uses PI controllers to regulate the d,q axis currents of the PMSM. A PI controller is also used for speed regulation (this produces the reference i_q^*). On the d axis, $i_d^* = 0$. Simulations are done at a sampling time of $100\ \mu s$. The model does not use a PWM state machine.

Since the implementation of the observer requires knowledge of the speed, in the simulation, the speed of the PMSM is measured and is fed in the observer. For an experimental implementation, an accurate speed signal could be obtained by, for example, differentiating the estimated rotor position yielded by the observer.

In the investigation, the motor is operated in speed control mode and is field-oriented with the correct rotor position right from the beginning of the motion (at start-up, $\theta_0 = 0$). The observer runs in parallel with the PMSM model; the estimates of the states are captured and are compared with the expected ones. The design gain in (8) is $k = 1000$.

Fig.1 shows the results of integration under ideal conditions (no dc offsets in measurements) – pure discrete-time integration is implemented corresponding to the transfer functions in Table II.

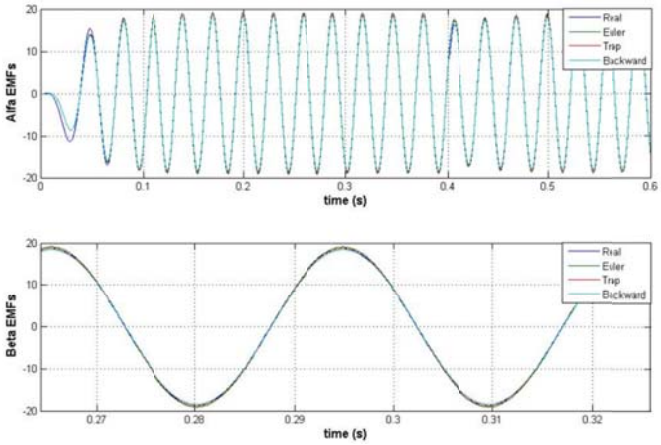

Fig. 1. Real versus estimated EMFs of the linear observer using the Euler, trapezoidal and backward integration methods

The speed of the PMSM is commanded to 1000 rpm and the drive runs at medium frequency (around 30 Hz). The motor starts against a load torque of 0.3 Nm and another 0.3 Nm are added at t=0.4s. The observer shown is implemented using the three integration methods proposed (in the simulation, there are three observers that run simultaneously).

Fig. 1 shows a comparison of the results; at this frequency, the estimated EMFs match the real ones irrespective of the integration method used – they all perform very well.

In conclusion, if only low/medium speed operation is intended, the simplest (or safest) integration method should be used; generally, the Euler method is preferred.

The three integration methods are compared again in Fig.2 where the PMSM drive is commanded to a speed of 5000 rpm; the corresponding frequency of the electrical signals is around 160 Hz. The load torque applied is the same.

Under these conditions, it is clear that the trapezoidal method outperforms the other two. The EMFs obtained from trapezoidal integration are closest to the real EMFs in both magnitude and phase.

Interestingly, the Euler method gives a waveform that leads the real EMF and whose magnitude is greater than real. To be exact, at 5000 rpm, with a sampling time of $100\ \mu s$, the lead angle is 16.2° and there is a 55% magnitude difference (150 V estimated instead of 95 V real).

The backward rectangular rule gives a waveform that lags the real EMF and has magnitude smaller than real. In Fig. 2, the lag angle is approximately 10.8° and the magnitude is 35% smaller than expected.

Note that if the EMFs obtained were used in a DFO scheme, the resulting lead or lag error angle of the estimates propagates in the estimated rotor position.

In conclusion, under ideal conditions, when high frequency signals are to be integrated, the trapezoidal method performs very well; results are accurate in both magnitude and phase.

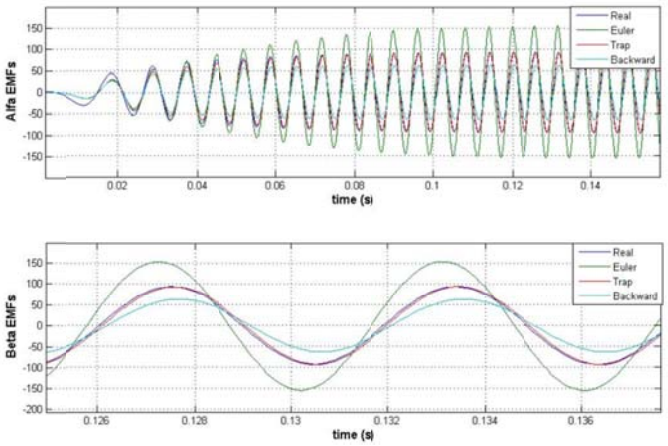

Fig. 2. Real versus estimated EMFs of the linear observer using the Euler, trapezoidal and backward integration methods at high frequency

Under real conditions, however, pure integration cannot be implemented. When the terms to be integrated contain measured signals, the ideal integrators must be replaced with the quasi-low pass filters which are of the form $\frac{1}{s+B}$.

The observer presented is simulated under these conditions in order to compare the performance of the three discretization

methods. The discrete transfer functions in Table III are used. The bandwidth of the filter is $20\,rad/s$ $(3.18\,Hz)$ - this is a typical value used in a real-time implementation.

Fig.3 shows the results when the drive operates at 1000 rpm. With all three methods, the estimated EMFs have slightly smaller magnitude (approximately 15%) than the real ones. More important, they are in phase with the real EMFs.

In conclusion, when quasi-low pass filtering is used, at medium frequency, the three discretization methods considered give comparable results and perform well.

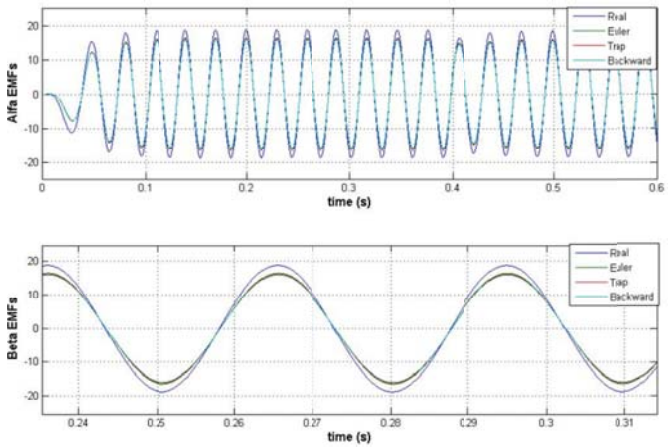

Fig. 3. Real vs. estimated EMFs with quasi-low pass filtering at low frequency

Finally, the results of integration at high frequency and with quasi-low pass filtering are shown in Fig 4. Under these conditions, none of the integration method proposed gives 100% accurate results.

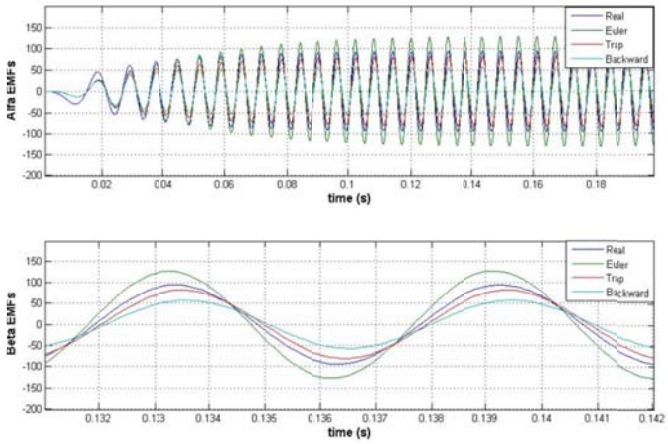

Fig. 4. Real vs. estimated EMFs with quasi-low pass filtering at high frequency

The Euler method yields a waveform that has 35% higher magnitude than real and is leading the real EMF by 8.4°. On the other hand, the backward rectangular rule gives an EMF that has a magnitude 40% lower than real and lags the real EMF by 12.6°.

The trapezoidal method is still the most accurate among the three: the waveform obtained is only 15% smaller in magnitude and lags the real EMF by 7.2°. However, note that this lag angle is pretty comparable with the lead angle of the Euler method and, under the circumstances; the high accuracy exhibited by the trapezoidal method at high frequency and with ideal integration (Fig. 2) is not maintained.

Note that if these waveforms are used to field-orient the PMSM, the Euler method will give a rotor position angle that leads the real rotor position by 8.4°while the trapezoidal method would give a position lagging by 7.2°- slightly better but not quite a big difference.

Some concluding remarks: the accuracy of discrete-time integration is influenced primarily by four factors: the sampling frequency, the frequency of the signals to be integrated, the filter's bandwidth and the integration (discretization) method used. With a fixed sampling time, the accuracy of integration worsens as the frequency of the signals increase.

When the estimates obtained are to be used in a high accuracy motor drive control algorithm, their magnitudes and phases may need corrected.

The phase of the estimates can be corrected (based on either theoretical or experimental methods) by mapping the lead/lag angle to the specific conditions (filter bandwidth used, sampling time, choice of integration method). The accuracy of the rotor position angle is an important performance factor in DFO drives (an accurate rotor position angle reduces oscillations and increases the region of stability of the drive).

The magnitude of the estimates needs to be corrected when they are directly used for feedback (for example, if the observer estimates the flux components of a motor and if the flux magnitude is controlled).

V. CONCLUSIONS

The paper discusses the problem of discrete-time integration of the equations of state observers and compares the accuracy of three integration methods at medium and at high frequency. Integration under ideal conditions (with pure integrators) and under real conditions (with quasi-low pass filters) is studied by considering a full-order observer for the permanent magnet synchronous motor. The Euler integration method, the trapezoidal method and the backward rectangular rule are compared. The paper finds that, under ideal conditions, at high frequency, the trapezoidal method gives very good results while the Euler and backward method are inaccurate in both magnitude and phase. Under real conditions, however, although it still performs the best, the trapezoidal method does not provide the expected accuracy – the lag angle of the estimates is better than that obtained with the backward method but is quite comparable with the lead angle yielded by the Euler method. The errors introduced by integration are relevant for direct field oriented motor drives running at high speed – for accurate control, the angle of the estimates should be corrected since the angle errors propagate in the estimated

rotor position. The errors associated with discrete-time integration depend on four factors: the frequency of the signals to be integrated, the sampling time, the bandwidth of the quasi-low pass filter and the discretization method used. At high frequency, for accurate control, a correction algorithm for the estimates may be needed.

REFERENCES

[1] P. Vas, "*Sensorless Vector and Direct Torque Control*", Oxford University Press, 1998.

[2] B.K Bose, *Modern Power Electronics and AC Drives*, Upper Saddle River, NJ, Prentice Hall 2002.

[3] Leonhard W. "*Control of Electrical Drives*" 2nd ed., 1996, Berlin, Germany, Springer-Verlag.

[4] T.M. Jahns "Motion Control with permanent magnet ac machines", Proc. Of the IEEE, Aug. 1994, vol. 82, pp.1241-1252.

[5] Finch J.W. and Giaouris D. (2008) "Controlled AC Electrical Drives", IEEE Transactions on Industrial Electronics, Vol. 55, No. 2, pp. 481-491.

[6] Kuo-Kai Shyu; Chiu-Keng Lai; Yao-Wen Tsai; Ding-I Yang, "A newly robust controller design for the position control of permanent magnet synchronous motor", IEEE Transactions on Industrial Electronics, Vol. 49, Issue 3, June. 2002, pp. 558 – 565.

[7] R. Monajemy, R. Krishnan "Control and dynamics of constant-power-loss operation of permanent magnet synchronous motor drive system" IEEE Transactions on Industrial Electronics, Vol. 48, Issue 4, Aug. 2001, pp. 839 – 844.

[8] Holtz J. (2006) "Sensorless control of induction machines – with or without signal injection ?" IEEE Transactions on Industrial Electronics, Vol. 53, No. 1, pp.7-30.

[9] Acarnley P.P., Watson J.F. "Review of Position-Sensorless Operation of Brushless Permanent-Magnet Machines", IEEE Transactions on Industrial Electronics, Vol. 53, No. 2, 2006, pp.352-362.

[10] Harnefors, L.; Jansson, M.; Ottersten, R.; Pietilainen, K. "Unified sensorless control of synchronous and induction motors" IEEE Transactions on Industrial Electronics, Vol. 50, Issue 1, Feb. 2003, pp. 153 – 160.

[11] Morimoto, S.; Kawamoto, K.; Sanada, M.; Takeda, Y. "Sensorless control strategy for salient pole PMSM based on extended EMF in rotating reference frame", IEEE Transactions on Industry Applications, Vol.38, Issue 4, July-Aug. 2002, pp. 1054 – 1061.

[12] Perera, P.D.C.; Blaabjerg, F.; Pedersen, J.K.; Thogersen, P "A sensorless, stable V/f control method for permanent-magnet synchronous motor drives", IEEE Transactions on Industry Applications, Vol. 39, Issue 3, May-June 2003, pp. 783 – 791.

[13] Jul-Ki Seok; Jong-Kun Lee; Dong-Choon Lee, "Sensorless speed control of nonsalient permanent-magnet synchronous motor using rotor-position-tracking PI controller", IEEE Transactions on Industrial Electronics, Vol. 53, Issue 2, April 2006, pp. 399 - 405

[14] M. Schroedl, "Sensorless control of AC machines at low speed and standstill based on the INFORM method", IEEE IAS Annual Meeting, Vol. 1, 1996, pp. 270-277.

[15] S. Ostlund, M. Brokemper, " Sensorless rotor-position detection from zero to rated speed for an integrated PM synchronous motor drive", IEEE Transactions on Industry Applications, Vol. 32, Issue 5, Sept-Oct. 1996, pp. 1158-1165.

[16] Y. Yamamoto, Y. Yoshida, T. Ashikaga "Sensorless control of PM motor using full order flux observer", IEEE Transactions on Industry Applications, Aug. 2004, Vol. 124, pp. 743-749.

[17] T. Batzel, K.Y. Lee, "Electric Propulsion with the Sensorless Permanent Magnet Synchronous Motor: Model and Approach", IEEE Transactions on Energy Conversion, Vol. 20, No. 4, Dec. 2005, pp.818-825.

[18] M. Comanescu, T.D. Batzel "Reduced order observers for rotor position estimation of nonsalient PMSM", 2009 IEEE International Electric Machines & Drives Conference, IEMDC 2009.

[19] L. Krichen, H.H. Abdallah, A. Ouali, "Reduced order observer for permanent magnet synchronous generator in wind energy conversion system", International Aegean Conference on Electric Machines and Power Electronics, 10-12 Sept. 2007, pp. 818-823.

[20] K. Tatematsu, D. Hamada, K. Uchida, S. Wakao, T. Onuki, "Sensorless control for permanent magnet synchronous motor with reduced order observer" Power Electronics Specialists Conference, 17-22 May 1998, vol. 1, pp. 125-131.

[21] Z. Yan, V. Utkin " Sliding Mode Observers for Electric Machines – An Overview", 28th Annual Conference of the Industrial Electronics Society, IECON '02, 5-8 Nov 2002, Vol.3, pp.1842 – 1847.

[22] S. Chi, Z. Zhang, L. Xu, " A novel sliding mode observer with adaptive feedback gain for PMSM sensorless vector control", Power Electronics Specialists Conference, PESC 2007, 17-21 June, pp. 2579-2585.

[23] C. Li, M. Elbuluk, "A Robust Sliding Mode Observer for Permanent Magnet Synchronous Motor Drives", IEEE IECON 2002,pp. 1014-1019.

[24] S. Bolognani, R. Oboe, M. Zigliotto, "Sensorless full digital PMSM drive with EKF estimator of speed and rotor position, IEEE Transactions on Industrial Electronics, Vol. 46, Feb. 1999, pp. 184-191.

[25] Huang, M.C, Moses, A.J, Anayi, F, Yao, X.G, "Reduced order linear Kalman filter theory in application of sensorless control for permanent magnet synchronous motor (PMSM)", 2006 IEEE Conference on Industrial Electronics and Applications", May 2006, pp. 1-6.

[26] K.D. Hurst, T.G. Habetler, G. Griva, F. Profumo "Zero-speed tacholess IM torque control: simply a matter of stator voltage integration" IEEE Transactions on Industry Applications, Vol. 34, Issue 4, 1998, pp.790-795.

[27] M. Comanescu, L. Xu "An improved flux observer based on PLL frequency estimator for sensorless vector control of induction motors" IEEE Transactions on Industrial Electronics, 2005, Vol. 53, pp. 50-56.

[28] G.F. Franklin, J.D. Powell, M. Workman *"Digital Control of Dynamic Systems"* Addison Wesley, 1998.

[29] Texas Instruments – TMS 320C2000 Microcontroller Digital Motor Control Libraries, http://focus.ti.com/mcu/docs